Aggregate Structures of Sorbed Humic Substances Observed in Aqueous Solution

P. A. MAURICE* AND
K. NAMJESNIK-DEJANOVIC

Department of Geology, Kent State University, Kent, Ohio 44242

Humic substances are high molecular weight, heterogeneous organic materials which dominate the natural organic matter pool in many aquatic environments and often form coatings on mineral surfaces. Humic substances sorbed to mineral surfaces may bind and hence immobilize trace metals, radionuclides, and nonionic organic pollutants, and they may also alter clay-mineral flocculation kinetics. Determining the physical shapes and forms of sorbed humic substances is essential for development of realistic pollutant-binding models. To this end, we are using direct, in-situ (in 0.01 M $CaCl_2$, $\leq$100 mg C L^{-1} solution, pH $\sim$5), nanometer-scale atomic force microscopy (AFM) to image the physical shapes and forms of humic substances sorbed to the basal-plane surface of mica. Under our experimental conditions, the sorbed molecules form ring-shaped aggregates with diameters on the scale of several tens of nanometers; smaller nanometer-scale rings present along the circumference could potentially represent hydrophobic domains. The highly porous three-dimensional copolymeric nature of the sorbed humic substances has important implications for reactivity at the soil particle-solution interface. Ongoing research focuses on determining the effects of changing solution conditions and sorbent properties on the shapes and forms of sorbed humic substances.

In many aquatic and terrestrial environments, the natural organic matter pool is dominated by humic substances (HS) in the form of fulvic acid (FA, water soluble at acidic to alkaline pH) and humic acid (HA, insoluble at acidic pH). These HS consist of an array of natural organic molecules, with average molecular weights on the order of a thousand daltons or more, and with variable aromaticity and functionality. When adsorbed to mineral surfaces, HS may bind and hence immobilize trace metals, radionuclides, and nonionic organic pollutants (*1*, *2*), and they may also alter clay-mineral surface charge properties (*3*) and flocculation kinetics (*4*). Determining the physical shapes and forms of adsorbed HS is essential for development of realistic pollutant-binding models, particularly with respect to partitioning of hydrophobic organic contaminants (*5*−*8*). The research described herein provided nanometer-scale images of HS sorbed to the muscovite basal-plane surface under conditions appropriate for many soil and surface-water environments (pH $\sim$ 5, 0.01 M $CaCl_2$ electrolyte, $\leq$ 100 mgC L^{-1}), opening new avenues of research in HS structure and sorption behavior.

A variety of intermolecular forces, such as electrostatic interactions, hydrogen bonding, hydrophobic interactions, and chelation with multivalent cations, can be expected to influence intermolecular association of individual HS molecules to form aggregates. Most of what we know about the shapes and forms of HS aggregates is based on indirect observations in solution or on imaging of dried samples (e.g. ref *9*). Schnitzer and his colleagues (*10, 11*) performed transmission electron microscopy (TEM) analysis on dried samples and showed that as HS concentration increased, small spheroids coalesce into flattened linear fibers; at high natural organic matter (NOM) concentrations, perforated sheetlike structures were observed. A similar suite of structures was observed by Namjesnik-Dejanovic and Maurice (*12*), using atomic-force microscopy (AFM) to image HS samples dried on mica surfaces. Buffle and colleagues (*13*, and references therein) reported small (1−3 nm diameter) "rigid globules" of HS at relatively low concentrations, using AFM imaging in air.

Although the studies referenced above provided high-resolution images, the aggregate structures (term used herein to describe the physical shapes and forms of coalesced HS molecules, or copolymers) of HS are likely to change upon drying (*10, 14*). Moreover, aggregate structures may well be different for molecules adsorbed to mineral surfaces than in solution because of interaction with the underlying mineral surface and with other adsorbed molecules. To determine directly the structures of sorbed HS aggregates, we have undertaken AFM imaging of HS adsorbed to mineral substrates, in air and aqueous solution. AFM is for the most part a nondestructive technique, and it allows for extremely high-resolution (molecular-scale) imaging of surfaces under environmentally relevant conditions (in air or aqueous solution) and with minimal sample preparation (no coating required). AFM provides information that is complementary to recently developed synchrotron-based in-situ techniques (*15*) because AFM permits increased resolution.

Experimental Section

To image HS by AFM, the HS must be firmly attached to a solid substrate by either adsorption (net accumulation at an interface, inherently two-dimensional) or precipitation (an accumulation to form a new solid phase, inherently three-dimensional) (*16*). For imaging in solution, electrolyte was added to enhance sorption (*17, 18*). Muscovite mica was chosen because freshly cleaved basal-plane surfaces contain large, molecularly flat areas, and because the basal-plane surface has a structure similar to that of most 2:1 clays. Moreover, an extensive AFM study of muscovite was conducted which allowed us to distinguish HS from potential dissolution/drying induced artifacts (*19*).

Imaging was conducted on a peat FA (NaOH extract, XAD-8 isolate from a muck layer) and water isolates (using XAD-8 macroporous resins (*20*) and reverse osmosis, RO) collected at a small freshwater wetland, McDonalds Branch basin in the New Jersey Pinelands (U.S.A.). The XAD-8 water isolate contained, by (operational) definition, both humic and fulvic acid fractions (*20*). Some of the XAD-8 and RO isolates had been freeze-dried, and these were redissolved in deionized, ultraviolet treated water prior to use. Others had never been freeze-dried; we saw no noticeable difference in samples due to previous freeze-drying.

* Corresponding author: phone: (330)672-2680; fax: (330)672-7949; e-mail: pmaurice@kent.edu

10.1021/es981113+ CCC: $18.00
Published on Web 03/16/1999

Tapping-mode AFM (TMAFM) imaging, which reduces lateral frictional forces during scanning and facilitates imaging of soft and easily deformed surfaces, was conducted using 100 μm Si_3N_4 tips and 125 μm TESP tips (characteristic resonant frequency 328 kHz) for imaging in solution and air, respectively. Imaging was conducted simultaneously in height (topographic), amplitude (essentially the first derivative of height data), and phase (sensitive to various surface properties such as viscoelasticity) modes. Height images in solution often had a slightly "fuzzy" appearance due to a combination of factors related to the softness of the scanned (HS) material; moreover, surface roughness of adsorbed (or precipitated) HS molecules resulted in an image display problem similar to depth-of-field limitations which made it difficult to display data with highly variable microtopography. Because amplitude mode results in flatter images but with enhancement of edges, this mode often resulted in the most easily interpretable structures. While phase imaging provided a means to differentiate portions of the surface covered by HS aggregates (softer and more viscoelastic) from the pristine mica surface (harder), it did not significantly enhance images of individual HS molecules and aggregates. Although some of the images shown here were collected in amplitude mode, height measurements were conducted on actual height mode images.

Results and Discussion

Figure 1a is an example of a TMAFM image in 0.01M $CaCl_2$ solution of a surface-water XAD-8 isolate. The structures shown in this image and in close-up Figure 1b are broadly typical of the samples we analyzed in $CaCl_2$ at pH ~5. The sample was prepared by applying a few drops of concentrated FA solution (1000 mg C L^{-1}, pH 4 in $CaCl_2$) to the mica surface and allowing the sample to sit for several hours under protective cover. It was then transferred while still damp into the AFM fluid cell, and 0.01 M $CaCl_2$ (pH ~5.5) was injected into the cell prior to imaging. We tried a wide variety of sample preparation techniques and found that this procedure was needed to promote sufficient strong adsorption for AFM imaging. We felt that it was a reasonable technique because HS can be expected to go through periodic wet-dry cycles in soils. We calculated that the final solution concentration in the fluid cell was ≤ 100 mg C L^{-1}. Cell volume was too small to permit measurement of pH and dissolved organic carbon concentration. The sample was allowed to sit for 2 h in the fluid cell prior to imaging, to permit the system to approach equilibration needed for image stability.

HS molecules appear aggregated into ring-shaped structures; not all of the rings are fully closed. Because of the thickness of the HS material, there is an inner diameter and an outer diameter for each ring (distance between these two diameters is defined as the interannular spacing, IAS). Ring diameters range from 30 to 70 nm with mean = 49 nm. Ring depth (height in z direction) is difficult to measure because the surface is not flat; estimated range = 1−10 nm and average depth (z direction) = 4 nm. The mean IAS of the rings = 23 nm, although this is likely to be an overestimate because the radius of curvature of the AFM tip tends to cause significant (to 100% or more in some cases) broadening of features at the nanometer scale, in the $x-y$ plane. In places (see close-up in Figure 1b), the IAS appear to contain smaller rings about 15 nm in diameter and with interior pore spaces of ≤10 nm. At least some of the larger scale rings appear to be made up of coalesced spheroids (~5 nm in diameter), although higher resolution images are needed to characterize the details of ring structure. We have observed similar ring structures during imaging in air of a peat fulvic acid isolate (from muck layer underlying the stream; Figure 2), although the rings tend to be flatter (see Table 1). The greater ring

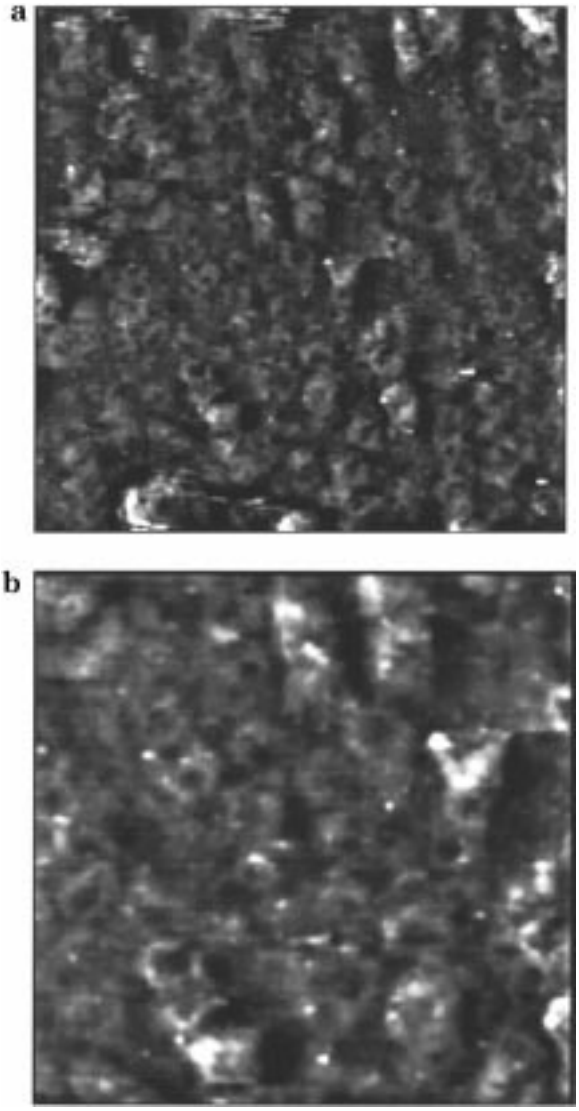

FIGURE 1. (a) Amplitude mode TMAFM image in solution of peat surface-water XAD-8 isolate on muscovite: 1.4 × 1.4 μm. Numerous ring structures are apparent. (b) Close-up of ring structure shown in (a): 700 × 700 nm. In some cases, larger-scale rings have small rings along their circumferences (within interannular spaces) (lower left corner).

width ($x-y$) and height (z) in solution suggests that the rings expand upward into the $CaCl_2$ containing solution, presenting smaller rings which could potentially represent hydrophobic domains, as postulated by Schulten et al. (*21*), along the circumference.

Our observations of ring structures are remarkably consistent with a model for NOM aggregate structure recently proposed by Schulten et al. (*21*, and references therein), based on numerous observations of the chemical and physical properties of HS (e.g. surface pressure, viscosity, analytical pyrolysis), including reactivity, and using geometrical optimization by molecular mechanics. Schulten et al. (*21*) performed "in-vacuo" modeling (wherein only HS molecules and no associated water molecules, electrolytes, or soil particle sorbents were included) of a humic polymer made up of 19 HA units each having molecular weight = 5541 DA. This modeling resulted in a thin ring with outer diameter ~40 nm, thickness (z-plane) = 5.7 nm, and with small (nm scale) diameter rings within the interannular spacings (around the circumference). The resulting aggregate thus exhibited nanometer-scale porosity. The materials

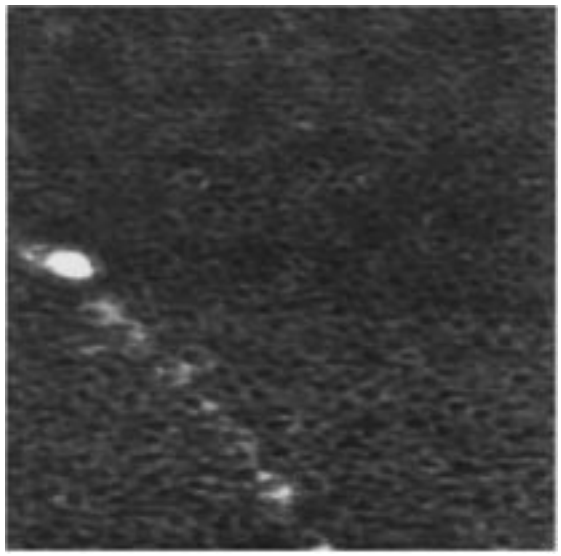

FIGURE 2. Height mode TMAFM image in air of peat fulvic acid isolate on muscovite: 1.25 × 1.25 μm. Maximum *z* range = 8.0 nm.

TABLE 1. Statistical Summary of Ring Dimensions

sample		ring diameter		interannular distance[b]		ring height	
muck extract	mean	35.3	mean	14.1	mean	0.65
HS imaged in air	STD	9.3	STD	3.4	STD	0.21
	min	19.6	min	7.0	min	0.2
	max	67.0	max	20.0	max	1.3
	N	100	N	100	N	100
aquatic HS imaged	mean	49.1	mean	22.9	mean	3.5
in $CaCl_2$ solution	STD	9.7	STD	6.3	STD	1.7
	min	30.1	min	9.0	min	1.1
	max	73.0	max	35.0	max	9.5
	N	25	N	25	N	25

[a] All measurements in nanometers. [b] Interannular distance = outer diameter of ring − inner diameter of ring. Note that interannular distance may be significantly increased (100% or more) due to the radius of curvature of the AFM tip, while other measurements are not subject to this tip broadening artifact.

imaged in our work have weight-average molecular weights of ~2200 Da (2150 for peat FA, 2170 for XAD-8 water isolate; determined by size exclusion chromatography, *22*). Hence, the individual molecules in our aggregate structure are less than half the molecular weight of those used in Schulten et al.'s (*21*) model. Moreover, in contrast to the "in vacuo" modeling, our molecules are hydrated, in either humid air or aqueous $CaCl_2$-containing solution, and are sorbed to the mica surface.

Gosh and Schnitzer (*9*) predicted that HS would behave as rigid spherocolloids at high HS concentration, low pH, or high neutral electrolyte concentrations but as flexible linear colloids at low HS concentrations (except at very low pH or high electrolyte concentrations). Stumm and Morgan (*23*) also predicted that in analogy with polysaccharides (*24*), a HS molecule in solution would have a coiled configuration and a small hydrodynamic radius at low pH and high ionic strength, but that the HS would extend further from the solid surface when adsorbed. Our images (Figure 1), which were collected at pH ~5 in 0.01 M $CaCl_2$, did not show either spherical structures or open linear structures but rather rings. Many polymeric materials have ring structures. Flexible, rodlike aggregates may assume a ring or "torus" shape if the two ends bend and join together, thereby eliminating energetically unfavorable regions at either end (*25*). Additional experiments are underway to determine whether the ring structure opens to form linear structures as pH is increased, electrolyte concentration is decreased, and a monovalent cation such as Na^+ is used in place of Ca^{2+}, and whether the structure closes into tight spheres as pH is further decreased.

The observed high porosity has profound implications for reactivity at the soil particle-solution interface and could help to explain previous observations of fast ionic exchange, rapid diffusion, and hydrophobic molecule partitioning (*6*, *7*, *9*) of HS. The smaller rings within the IAS could potentially represent hydrophobic domains, which could be important for the partitioning of hydrophobic organic compounds (*5*). At the present time, we do not know whether these pores are hydrophobic in nature. High porosity would permit interaction between the underlying mineral surface and the surrounding aqueous solution, so that, for example, organic coatings probably would not significantly retard mineral dissolution rates (*26*, *27*). Additional research to determine changes in aggregate structure as a function of solution conditions (HS concentration, pH, ionic strength, cation identity) is underway.

Acknowledgments

We thank the National Sciences Foundation (NSF-EAR 9628461 to P.A.M.) for funding. We thank S. Traina and S. Cabaniss for helpful discussion, Y.-P. Chin for molecular weight measurements, and several anonymous reviewers for detailed review comments. P. M. dedicates this manuscript to W. Stumm in grateful thanks for his encouragement of female environmental chemists.

Literature Cited

(1) Cabaniss, S. E. *Environ. Sci. Technol.* **1990**, *24*, 583.
(2) Schroth, B. K.; Sposito, G. *Environ. Sci. Technol.* **1998**, *32*, 1404.
(3) Tipping, E.; Cooke, D. *Geochim. Cosmochim. Acta* **1982**, *46*, 75.
(4) Liang, L.; Morgan, J. J. In *Chemical Modeling of Aqueous Systems II*; American Chemical Society: Washington, DC, 1990; pp 293−308.
(5) Pignatello, J. J. *Adv. Colloid Int. Sci.* **1998**, *76*−*77*, 445.
(6) Chiou, C. T.; Peters, L. J.; Freed, V. H. *Science* **1979**, *206*, 831.
(7) McCarthy, J. F.; Zachara, J. M. *Environ. Sci. Technol.* **1989**, *23*, 496.
(8) Schlautmann, M. A.; Morgan, J. J. *Environ. Sci. Technol.* **1993**, *27*, 961.
(9) Ghosh, K.; Schnitzer, M. *Soil Sci.* **1980**, *129*, 266.
(10) Chen, Y.; Schnitzer, M. In *Humic Substances II*; Hayes, M. H. B., MacCarthy, P., Malcolm R. L., Swift R. S., Eds.; John Wiley & Sons Ltd.: New York, 1989; pp 622- 646.
(11) Stevenson, I. L.; Schnitzer, M. *Soil Sci.* **1982**, *133*, 179.
(12) Namjesnik-Dejanovic, K.; Maurice, P. A. *Colloids Surf. A* **1997**, *120*, 77.
(13) Buffle, J.; Wilkinson, K. J.; Stoll, S.; Filella, M.; Zhang, J. *Environ. Sci. Technol.* **1998**, *32*, 2887−2899.
(14) Leppard, G. G.; Burnison, B. K.; Buffle, J. *Anal. Chim. Acta* **1990**, 232.
(15) Myneni, S. B.; Brown, J. T.; Meyer-Ilse, W.; Martinez, G. A.; Hussain, Z.; Warwick, A. *ACS Environmental Chemistry Preprints Extended Abstracts* **1998**, *38*, 57.
(16) Sposito, G. *The Surface Chemistry of Soils*; Oxford University Press: New York, 1994; p 234.
(17) Dempsey, B. A.; O'Melia C. R. In *Aquatic and Terrestrial Humic Materials;* Christman, R. F., Gressing, E. T., Eds.; Ann Arbor Sci.: Ann Arbor, MI, 1983; pp 239−273.
(18) Tipping, E. *Geochim. Cosmochim. Acta* **1981**, *45*, 191.
(19) Johnsson, P. A.; Hochella, M. F., Jr.; Parks, G. A.; Blum, A. E.; Sposito, G. In *Water-rock Interaction: VII;* Kharaka, Y. K., Maest, A. S., Eds.; A. A. Balkema: Rotterdam, 1992; pp 159−162.
(20) Aiken, G. R. In *Humic substances in Soil, Sediment, and Water;* Aiken, G. R., McKnight, D. M., Wershaw, R. L., MacCarthy, P., Eds.; John Wiley & Sons Ltd: New York, 1985; pp 363−386.
(21) Schulten, H.-R.; Leinweber, P.; Schnitzer, M. In *Structure and Surface Reactions of Soil Particles*; Huang, P. M., Senesi N., Buffle, J., Eds.; John Wiley & Sons Ltd: New York, 1998; p 281.
(22) Chin, Y.-P.; Aiken, G. R.; O'Loughlin E. *Environ. Sci. Technol.* **1994**, *28*, 1853.

(23) Stumm, W.; Morgan, J. *Aquatic Chemistry*; John Wiley & Sons: New York, 1996; Chapter 9.
(24) Yokoyama, A.; Srinivasan, K. R.; Fogler, H. S. *Langmuir* **1989**, *5*, 534.
(25) Israelachvili, J. N. *Intermolecular and Surface Forces*, 2nd ed.; Academic Press: London, 1992.
(26) Maurice Johnsson, P. A. Ph.D. Dissertation, Stanford University, 1993.
(27) Nugent, M. A.; Brantley, S. L.; Pantano, C. G.; Maurice, P. A. *Nature* **1998**, *395*, 588.

Received for review October 29, 1998. Revised manuscript received February 16, 1999. Accepted February 24, 1999.

ES981113+